British Journal of Pharmacology (2000) 131, 1689–1699

www.nature.com/bjp

Bradykinin regulation of salt transport across mouse inner medullary collecting duct epithelium involves activation of a Ca^{2+}-dependent Cl^- conductance

[1]H. Kose, [1]S.H. Boese, [1]M. Glanville, [1]M.A. Gray, [1]C.D.A. Brown & *,[1]N.L. Simmons

[1]Department of Physiological Sciences, Medical School, Framlington Place, University of Newcastle upon Tyne, Newcastle upon Tyne NE2 4HH

1 The mechanism by which bradykinin regulates renal epithelial salt transport has been investigated using a mouse inner medullary renal collecting duct cell-line mIMCD-K2.

2 Using fura-2 loaded mIMCD-K2 cells bradykinin (100 nM) has been shown to induce a transient increase in intracellular Ca^{2+} *via* activation of bradykinin B2 receptors localized to both the apical and basolateral epithelial cell surfaces.

3 In mIMCD-K2 epithelial cell-layers clamped in Ussing chambers, 100 nM bradykinin *via* apical and basolateral bradykinin B2 receptors stimulated a transient increase in inward short-circuit current (I_{sc}) of similar duration to the increase in intracellular Ca^{2+}.

4 Replacements of the bathing solution Na^+ by the impermeant cation, N-methyl-D-glucamine and of Cl^- and HCO_3^- by the impermeant anion gluconate at either the apical (no reduction) or basal bathing solutions (abolition of the response) are consistent with the bradykinin-stimulated increase in inward I_{sc} resulting from basal to apical Cl^- (anion) secretion.

5 Using the slow whole cell configuration of the patch-clamp technique, bradykinin was shown to activate a transient Cl^- selective whole cell current which showed time-dependent activation at positive membrane potentials and time-dependent inactivation at negative membrane potentials. These currents were distinct from those activated by forskolin (CFTR), but identical to those activated by exogenous ATP and are therefore consistent with bradykinin activation of a Ca^{2+}-dependent Cl^- conductance.

6 The molecular identity of the Ca^{2+}-dependent Cl^- conductance has been investigated by an RT–PCR approach. Expression of an mRNA transcript with 96% identity to mCLCA1/2 was confirmed, however an additional but distinct mRNA transcript with only 81% of the identity to mCLCA1/2 was identified.

British Journal of Pharmacology (2000) **131,** 1689–1699

Keywords: Inner medullary collecting duct; IMCD; bradykinin; renal epithelial salt transport, Cl^- secretion; Ca^{2+}-dependent Cl^- conductance; CFTR

Abbreviations: CFTR, cytic fibrosis conductance regulator; IMCD, inner medullary collecting duct; I_{sc}, short-circuit current; MDCK, Madin Darby Canine Kidney (cells); mCLCA1 (mCACC), murine Ca^{2+}-dependent Cl^- conductance gene; R, ratio of fura-2 fluorescence emission (<510 nm) intensities at excitation wavelengths of 350 and 380 nm

Introduction

The renal kallikrein–kinin system plays a significant role in the regulation of salt and water excretion, renal infusion of kinins being associated with increased urinary sodium chloride and water excretion (Margolius, 1984). Kallikrein is produced in the cells of the connecting tubule and cortical collecting duct, kininogen substrate being present in the cortical and medullary collecting duct cells (Vio *et al*., 1998). Bradykinin binding sites (B2) are present at both cortical and medullary collecting duct cells and on medullary interstitial cells (Schanstra *et al*., 1999). Blockade of the renal bradykinin B2 receptor by the long-lasting antagonist, HOE 140, in dogs has an antidiuretic and antinatriuretic action (Siragy *et al*., 1997). Mukai *et al*. (1996) using microcatheterization studies in rats, further showed that HOE-140, *in vivo*, increases Cl^--reabsorbtion along the medullary collecting duct. This data suggests that endogenous activation of bradykinin B2 receptors increases Cl^- excretion to urine at the collecting duct.

Detailed studies of salt transport in the inner medullary collecting duct (IMCD) show that electrogenic Na^+ absorption occurs together with Cl^- secretion and both processes participate in the regulation of overall NaCl balance (Rocha & Kudo, 1990a,b; Zeidel, 1993; Husted *et al*., 1995; 1998; Husted & Stokes, 1996; Kizer *et al*., 1995). Bradykinin B2 receptors have been localized to both the apical and basal membranes of both cortical and medullary collecting ducts (Figueroa *et al*., 1995) and studies using primary cultures of pig renal papillary collecting duct cells (Cuthbert *et al*., 1985), or an established dog kidney cell-line, MDCK (Simmons, 1992) show that electrogenic ion transport may be stimulated from both the apical and basal epithelial surfaces by kinins. Despite the clear location of bradykinin B2 receptors to collecting duct epithelial cells, there is still uncertainty regarding the precise cellular basis of the renal epithelial response to kinins. Although it is clear that short-circuit current responses are Cl^- dependent, both inward and

*Author for correspondence; E-mail: n.l.simmons@ncl.ac.uk

outward currents were noted by Cuthbert *et al.* (1985). Similarly, activation of enhanced Cl^- secretory currents in MDCK cells were judged to be secondary to activation of a basolateral K^+ conductance (Simmons, 1992).

In order to study the cellular basis of the response of renal collecting duct cells to kinins we have chosen an inner medullary collecting duct cell line (mIMCD-K2) established from the initial outer portion of the inner medulla, from a mouse transgenic for SV40 (Kizer *et al.*, 1995). This cell-line allows the reconstitution of functional epithelia *in vitro* and macroscopic trans-epithelial currents may be correlated with ion channel activation by renal-acting hormones and parcrines using patch-clamp methodology (Vandorpe *et al.*, 1995; 1997; Boese *et al.*, 2000). mIMCD-K2 epithelia retain features typical of the IMCD; for instance a mineralocorticoid-sensitive net Na^+ absorption inhibited by amiloride (Kizer *et al.*, 1995) and mediated *via* apical cyclic nucleotide gated cation channels (Vandorpe *et al.*, 1997). Importantly, this cell-line displays electrogenic Cl^- secretion (Kizer *et al.*, 1995) after stimulation by agents that raise intracellular cyclic AMP. This Cl^- secretion is mediated by apical expression of CFTR (Schwiebert *et al.*, 1994; Vandorpe *et al.*, 1995). Recently we have reported co-expression of a calcium activated Cl^- channel together with CFTR in mIMCD-K2 cells (Boese *et al.*, 2000). Since a number of stimuli, including kinins, may mobilize intracellular Ca^{2+} in IMCD (Zeidel, 1993), the possible regulation of the calcium activated Cl^- channel and its importance to the cellular response to bradykinin has been assessed.

Methods

Cell culture

mIMCD-K2 cells (Kizer *et al.*, 1995) were kindly provided by Dr B. Stanton (Dartmouth Medical School, Hanover, NH, U.S.A.). mIMCD-K2 cells were routinely cultured (18–25 serial passages) in Opti-MEM 2 mM l-glutamine and 30 μg ml^{-1} gentamycin with 10% v v^{-1} foetal bovine serum at 37°C in an air : 5% CO_2 gas mixture. Stock Roux bottles (75 cm^2 growth area) were coated with Vitragel : Cellon collagen and cells were passaged by trypsinisation (2 ml of 0.5% w v^{-1} trypsin, 0.7 mM EDTA in Ca^{2+} and Mg^{2+} free saline) to form a cell suspension and culturing at a 1 : 10 split ratio. Functional epithelial layers of mIMCD-K2 cells were prepared by high-density seeding (2×10^5 cells cm^{-2}) onto collagen-coated permeable filter supports (Snapwell, Costar, 12 mm diameter, 0.4 μm pore diameter). Filter supports were then cultured in 6-well plates at 37°C, 5% CO_2 for 7–25 days with medium replacement every 2–3 days. For patch-clamp recording cells were seeded at low density (1×10^4 cells) onto coverslips (25 mm diameter) and cultured as for filter supported layers.

Measurements of short-circuit current and epithelial resistance

Cultured epithelial layers were mounted in Ussing type chambers maintained at 37°C, connected to an automatic voltage clamp (WPI Instruments, DVC-1000, New Haven CT, U.S.A.) *via* KCl-agar salt-bridges and reversible electrodes (Ag : AgCl for current passage, calomel for voltage sensing) and measurements of open-circuit electrical p.d., transepithelial resistance, and short-circuit current (I_{sc}) made in modified Krebs solutions.

Whole-cell patch clamp analysis

Cultured mIMCD-K2 cells grown on coverslips were transferred to the stage of an inverted microscope for patch-clamp recording. The chamber volume was approximately 0.5 ml and the cells were perfused continuously at 5 ml min^{-1}. The nystatin slow whole-cell configuration of the patch-clamp technique (Hamill *et al.*, 1981) was used to measure membrane currents. Experiments were performed at room temperature. Pipettes were pulled from borosilicate glass and had resistances, after fire polishing, of 3–6 MΩ. Seal resistances were typically between 5–20 GΩ.

Whole-cell currents were measured with an EPC9 patch-clamp amplifier (Heka Electronics, Germany) using the following protocol: The cell was clamped to a holding potential of 0 mV and the current responses to depolarizing and hyperpolarizing voltage pulses were measured. Voltage stimulation and data acquisition were achieved using 16-bit DA and AD converters (ITC-16, Instrutech, U.S.A.), controlled by a PC, using the Pulse software (Heka Electronics, Germany). Data were filtered at 1 kHz and sampled at 2 kHz and stored on the computer hard disk. Data were analysed using PulseFit and PulseTools (Heka Electronics, Germany). The slope conductance was obtained by linear regression of the mean current values at 0.5–1.0 s averaged from voltage steps (held for 1 s) to +80 mV and −80 mV in 20 mV increments. Reversal potentials were determined from voltage ramps from −80 mV to +80 mV.

Measurements of intracellular Ca^{2+}

mIMCD-K2 cells grown as epithelial monolayers were loaded by incubation with 10 μM Fura-2 AM in both apical and basal bathing solutions in standard growth media for 35–60 min at 37°C, in a 5% CO_2 : 95% air-gas mixture. The epithelial layers were then placed in a 24 mm diameter perfusion chamber allowing perfusion of both apical and basal bathing solutions fitted to the stage of an inverted Nikon Diaphot fluorescence microscope. The cells were imaged using a long working distance objective lens (Nikon Fluor 60/0.7 Ph3DM, 160 mm working distance), and perfused continuously (bath volume apical 0.5 ml, basal solution 1 ml perfusion at 5 ml min^{-1}).

Changes in intracellular Ca^{2+} were determined by measuring the fluorescence of Fura-2 loaded cells with a dual wavelength excitation micro-spectrofluorimeter (Newcastle Photonics, U.K.). Groups of cells (5–10) were alternately illuminated with excitation light at 340 nm and 380 nm (cycle time 1.2 s), and emitted light was filtered using a 510 nm long-pass filter. Fluorescence data were corrected for cell autofluorescence (typically 5% of Fura intensity) using an unloaded cell layer and the emission ratio at the two excitation wavelengths of 350 and 380 nm (R) was determined as an index of intracellular Ca^{2+} (Grynkiewicz *et al.*, 1985).

Expression and identity of mCLCA1 mRNA-related transcripts by reverse transcription-polymerase chain reaction

Confluent cell layers were washed (×3) with phosphate buffered saline (mM: PBS 2.7, KCl 1.47, KH_2PO_4 135, NaCl 8, $Na_2HPO_4.7H_2O$). Lysis buffer (5 ml, 200 mM; NaCl, 200 mM; tris-HCl pH 7.5, 1.5 mM; $MgCl_2$, 4.7 μM; disodium EDTA; 2%; SDS, 1 μg proteinase K) was added and layers incubated for 5–10 min at 20°C. The resultant lysate was

titurated through a 21-gauge needle, transferred to a 20 ml universal tube and incubated at 45°C for 1 h. Sodium chloride was added to a final concentration of 300 mM before re-suspension, as above.

mRNA was purified from total RNA by the use of an oligo-dT resin method (Pharmacia Biotech, St. Albans, Herts, U.K.). Poly-A^+ RNA was precipitated by the addition of 40 μl of 3M sodium acetate pH 5.2 (Sigma) and 1 ml of 100% ethanol (BDH, Analar). After centrifugation ($30{,}000 \times g$ for 1 h at 4°C), the solution was decanted and the pellet air-dried for 5 min before adding 100 μl of Tris-HCl pH 8.5. This was incubated at 65°C for 10 min to aid dissolution. Purity and yield of mRNA was assessed by $A_{260\,nm}$ and $A_{280\,nm}$.

Samples of poly-A^+ RNA (1 μg) were incubated with RT buffer ((mM) Tris-HCl 50, pH 8.3, KCl 50, $MgCl_2$ 4, DTT 10, MBI Fermentas), 0.5 mM dNTPs (MBI Fermentas), 10 units Moloney murine leukemia virus reverse transcriptase (M-MuLV RT MBI Fermentas), 20 units RNA-ase inhibitor (MBI Fermentas) and 0.023 units random hexamer primers (Pharmacia Biotech). Total volume was 20 μl, made with water (molecular biology grade, BDH), and incubation was at 42°C for 1 h. Negative controls were included where M-MuLV RT was omitted to discount false positives due to DNA contamination.

cDNAs (2.5 μl in a 25 μl PCR reaction) were incubated with PCR buffer (10 mM tris-HCl pH 8.8, 50 mM NaCl, 0.08% Nonidet P40, MBI Fermentas), 2 mM $MgCl_2$ (MBI Fermentas), 0.2 mM dNTPs, 1.25 units recombinant *Taq* DNA polymerase (MBI Fermentas), 0.5 μM forward and reverse primers and molecular biology grade water (BDH). PCR was performed using the PCR Express Thermal Cycler (Hybaid) for 30 amplification cycles. Each cycle consisted of 94°C for 30 s, 55°C for 30 s, and 72°C for 1 min. Oligonucleotide primers for mCLCA1 (mCACC) were from the published mouse mCLCA1 sequence; forward primer 5′-GCCTCCATAATGTTCATGC-3′, reverse primer, 5′-CCGGAAGTGCTCGGTCAC-3′ as described by Gruber *et al*. (1998b). PCR products were analysed using agarose gel electrophoresis of PCR mixtures using ethidium bromide fluorescence to visualize products. Appropriate gel bands were excised from the gel and cloned using the TA cloning vector pCR2.1 TOPO (Invitrogen). The identity of the cloned PCR products were determined by automatic sequencing using fluorescent di-deoxy dye-termination on an ABI Prism model 377 automated sequencer. Comparison of the identity of the cloned PCR fragments to published sequence was performed using BLASTN (www.ncbi.nlm.nih.gov) (Altschul *et al*., 1997). Multiple sequence alignment was performed as described by Corpet (1988).

Solutions

A modified Krebs' solution was used for I_{sc} measurements of epithelial layers; its composition was (all mM): NaCl 125, KCl 5.4, $CaCl_2$ 2.8, $MgSO_4$ 1.2, KH_2PO_4 1.5, $NaHCO_3$ 20, glucose 5, pH 7.4 at 37°C) gassed continuously with a gas mixture of 95% O_2 and 5% CO_2. A Na^+-free solution was prepared as above except NaCl and $NaHCO_3$ were replaced by N-methyl-D-glucamine and the solution titrated by HCl. A Cl^- and HCO_3^- free medium was obtained by replacement of NaCl, $NaHCO_3$ and KCl by their gluconate salts and buffering with Tris-HEPES(10), pH 7.4.

For patch-clamp and intracellular Ca^{2+} recordings the bath solution contained (in mM) NaCl 140, KCl 4.5, KH_2PO_4 1, $MgCl_2$ 1, $CaCl_2$ 2, HEPES 10, tris(hydroxymethyl)amino-methane (TRIS) 6, glucose 5. The pH was adjusted to 7.4 by addition of TRIS. A 10 fold reduction in [Cl^-] was obtained by replacement of NaCl with NaAspartate and a 10 fold increase in [K^+] was obtained by replacement of NaCl by KCl. All bath solutions were adjusted to 320 mosmol kg^{-1} H_2O. by addition of 20 mM sucrose to avoid activation of swelling-sensitive currents (Boese *et al*., 2000). The pipette solution contained (in mM): NaCl 10, KCl 130, $MgCl_2$ 2, HEPES 10 and nystatin (100–200 μg ml^{-1}). The pH was adjusted to 7.2 by addition of TRIS. The osmolarity of the pipette solution was 300 mosmol kg^{-1} H_2O.

Materials

Forskolin (Sigma Chemical Co.) was made as a stock solution in ethanol (10^{-2} M) and used at 10 and 0.1–1 μM (respectively). Bradykinin was made as a stock solution in Krebs' solution at 1 mM. B1, [Des-Arg^9]-bradykinin and B2-selective [Hyp^3]-bradykinin agonists and the antagonist HOE-140 were from Research Biochemicals International. Fura-2 AM was from Molecular Probes Inc, Oregon, U.S.A. Culture media and other chemicals used were from Sigma and were of the highest purity available.

Statistics

Data are expressed as mean values ± s.e.mean for n separate epithelial layers or cells. Significance of difference between mean values was determined using ANOVA with Bonferroni-corrections for multiple comparisons applied to Student's t-test (unpaired data) for tests between individual data pairs (where appropriate). The level of significance was set at $P \leqslant 0.05$.

Results

Bradykinin mobilisation of intracellular [Ca^{2+}]$_i$

Figure 1 shows the effect of perfusion of either the apical or basal surfaces of mIMCDK2 epithelial monolayers with

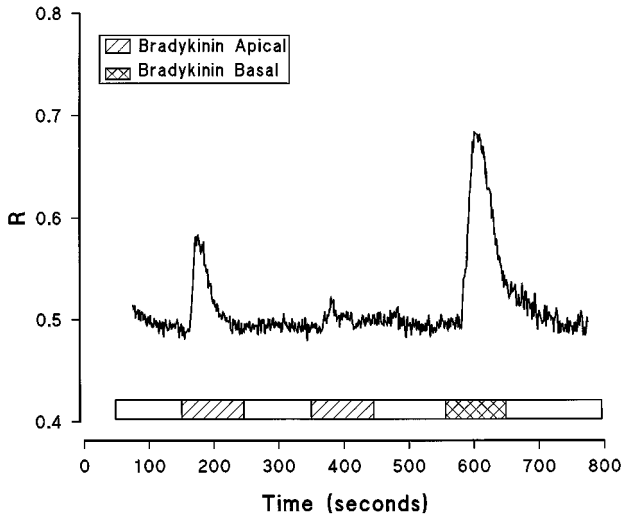

Figure 1 Representative trace showing the effect of apical and basal application of bradykinin (100 nM) upon intracellular Ca^{2+} as measured by the fluorescence emission ratio, R (see methods) in mIMCD-K2 epithelial layers. Epithelial layers were clamped in a perfusion chamber allowing perfusion of either apical or basal solutions.

100 nM bradykinin. Apical bradykinin results in a prompt increase in $[Ca^{2+}]_i$ as indicated by an increased fluorescence ratio, R (mean increase from 0.45 ± 0.02 to peak values of 0.63 ± 0.04 ($n=14$), $P<0.01$). There is marked desensitization of the response to bradykinin during exposure (Figure 1), furthermore repeated addition of apical bradykinin is associated with a marked decline in the subsequent response (Figure 1). Upon exposure of the basal surface to 100 nM bradykinin, despite desensitization of the apical response, there is a prompt increase in R. This data confirms the existence of functional bradykinin receptors at both epithelial domains of mIMCDK2 cells coupled to mobilization of intracellular $[Ca^{2+}]_i$. The response to apical bradykinin was dose related; with single additions 1 nM bradykinin increased the R by 0.048 ± 0.002, 10 nM bradykinin by 0.091 ± 0.026 and after 100 nM bradykinin by 0.163 ± 0.016 (all $n=4$). Addition of the bradykinin B2 receptor-selective agonist [Hyp^3]-bradykinin at 100 nM to the apical perfusate also increased the R from 0.5 ± 0.01 to 0.67 ± 0.03, $n=5$, $P<0.01$, whereas the addition of 100 nM of the bradykinin B-receptor selective agonist Des-Arg^9 bradykinin was without substantial effect (R prior to addition 0.52 ± 0.01, after addition 0.54 ± 0.01, $n=5$, n.s.). Pre-exposure of the apical surface of cell monolayers to 100 nM of the selective bradykinin B2-antagonist HOE-140 (Wirth *et al*., 1991) did not itself increase intracellular $[Ca^{2+}]_i$ but completely blocked the response to 100 nM bradykinin (R prior to BK, 0.46 ± 0.01, post BK 0.46 ± 0.01, $n=3$). Similar data were observed for basolateral additions of the B1/B2 selective agonists suggesting that B2-kinin receptors are present at both apical and basal epithelial plasma membrane domains (not shown). Figure 2 shows that exogenous apical ATP (100 μM) increases the R, consistent with expression of purinoreceptors in this cell-line (McCoy *et al*., 1999) and that depletion of intracellular Ca^{2+} stores by exposure to 5 μM thapsigargin eliminates the bradykinin-dependent increase in R consistent with a PLC/IP$_3$ dependent mechanism.

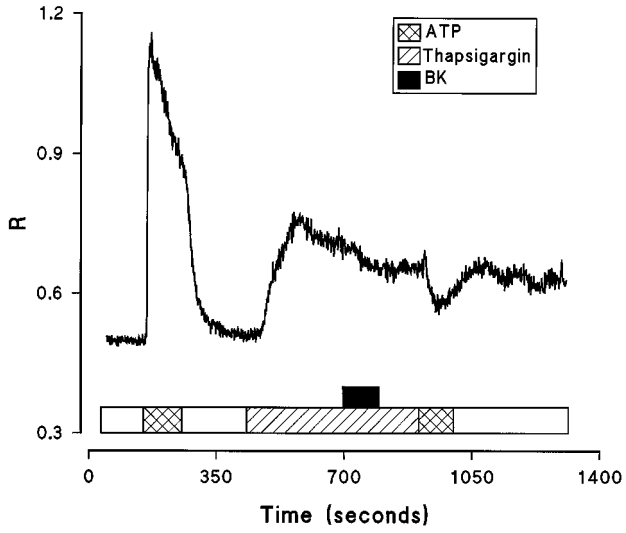

Figure 2 The effect of depleting intracellular Ca^{2+} stores by incubation in 5 μM thapsigargin upon the response of the fluorescence emission ratio, R, to apical perfusion with 100 nM bradykinin. An exposure to 100 μM apical ATP, as a control for agonist activation of Ca^{2+}, preceded thapsigargin exposure.

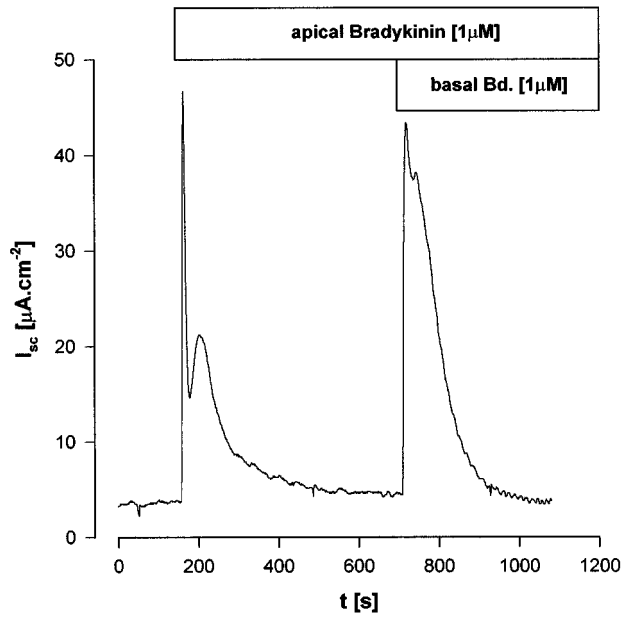

Figure 3 Representative trace showing the effect of bradykinin (1 μM) applied to the apical or basal bathing solutions upon inward I_{sc}.

Kinin stimulation of inward I_{sc} in mIMCD-K2 cells

Figure 3 shows the effect of bradykinin addition to either the apical or basal bathing solution of voltage-clamped mIMCD-K2 monolayers mounted in Ussing-type chambers upon I_{sc}. Addition of 100 nM bradykinin to either bathing solutions consistently stimulated I_{sc}, although the magnitude of the peak response varied between batches of epithelial monolayers. In this group of experiments addition of 100 nM bradykinin to the apical bathing solution stimulated inward I_{sc} from 3.8 ± 0.5 μA cm^{-2} to a peak value of 28.5 ± 4.9 μA cm^{-2} ($n=10$). The response is multiphasic, a rapid transient being followed by a secondary peak. This may result from initial release of Ca^{2+} from stores followed by enhanced Ca^{2+} entry at the plasma membrane. Desensitization of the response to bradykinin occurs despite the continued presence of bradykinin, I_{sc} values falling towards control values after 6 min (Figure 3). Apical desensitization does not alter the subsequent I_{sc} response to addition of bradykinin to the contralateral chamber (Figure 3); in this series of 10 monolayers inwards I_{sc} was stimulated by 100 nM bradykinin from 3.2 ± 0.3 μA cm^{-2} to a peak value of 40.1 ± 3.8 μA cm^{-2}. As with apical addition, there is rapid desensitization of the I_{sc} response to bradykinin applied to the basal bathing solution despite the continued presence of the agonist (Figure 3), values 6 min post addition being similar to pre-stimulation values. The time-course of the I_{sc} response to bradykinin, and the occurrence of bradykinin responses from both epithelial surfaces mirror the observed change in $[Ca^{2+}]_i$ (Figure 1).

Addition of 100 nM of the B1-specific agonist [Des-Arg^9]-bradykinin to either epithelial surface was without significant effect upon I_{sc} (apical addition, control I_{sc} 3.8 ± 1.4 μA cm^{-2}, plus [Des-Arg^9]-bradykinin, 6.7 ± 3.9 μA cm^{-2}, $n=4$, n.s.; basal addition, control I_{sc} 3.4 ± 1.1 μA cm^{-2}, plus [Des-Arg^9]-bradykinin, 3.5 ± 0.9 μA cm^{-2}, $n=4$, n.s.). In contrast addition of 100 nM B2-specific agonist [Hyp^3]-bradykinin to both bathing solutions markedly stimulated a transient increase in I_{sc} (control I_{sc} 3.8 ± 1.2 μA cm^{-2}, plus apical [Hyp^3]-bradykinin, 14.7 ± 1.6 μA cm^{-2}, control 3.0 ± 0.9 μA cm^{-2}, plus basal [Hyp^3]-bradykinin, 22.9 ± 1.9 μA cm^{-2}, all $n=6$). Pre-addition of the B2-specific antagonist Hoe-140

(100 nM) abolished the response to bradykinin ($n=3$). This data is therefore consistent with the existence of B2 receptors mediating stimulation of electrogenic ion transport in mIMCD-K2 epithelial mediated *via* increased $[Ca^{2+}]_i$.

Ionic basis of the bradykinin-stimulated I_{sc}

The bradykinin-stimulated increase in I_{sc} is not abolished by replacement of apical bathing solution Na^+ or anion content (Cl^- or HCO_3^-); in separate epithelial layers, the maximum control increment in I_{sc} plus apical 1 μM bradykinin was 6.1 ± 1.8 μA cm^{-2}, $n=4$, after total Na^+ replacement of the apical solution by N-methyl-D-glucamine, the increment was 9.73 ± 0.6 μA cm^{-2}, $n=3$ and after replacement of the Cl^- and HCO_3^- content the increment was 11.1 ± 1.1 μA cm^{-2}, $n=4$ (n.s. $P>0.05$). In both situations of apical ion replacement, the transepithelial chemical gradients would favour electrogenic anion exit across the apical membrane. In contrast to apical ionic replacement there was abolition of the bradykinin-stimulated increment upon replacement of the basal bathing solution Na^+ ($n=4$, $P<0.05$) and Cl^- together with HCO_3^- ($n=4$, $P<0.05$). Taken together, this data is consistent with bradykinin stimulation of basal to apical anion secretion dependent upon the presence of Na^+ in the basal bathing solution.

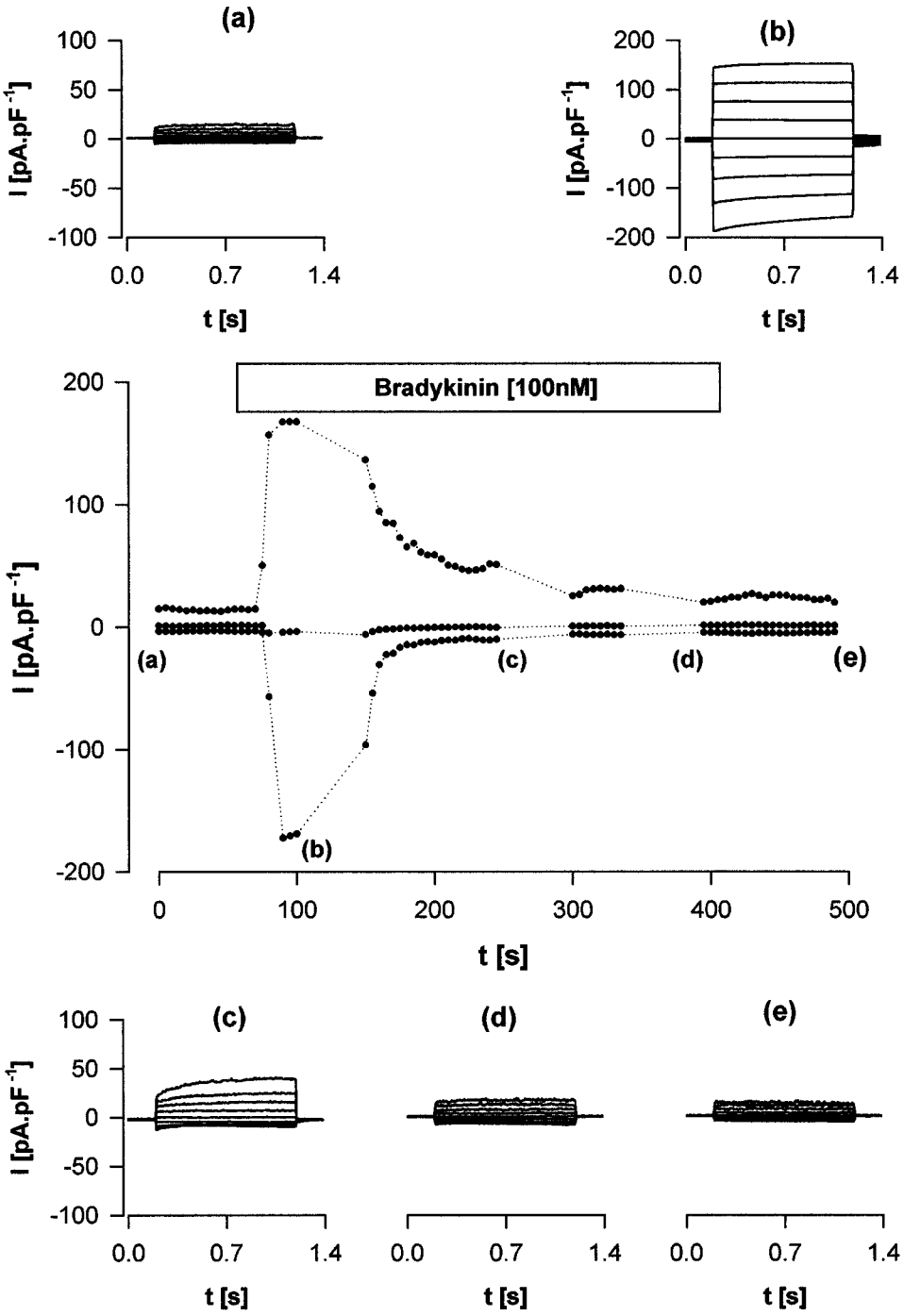

Figure 4 The effect of bradykinin (50 nM) on whole cell current (I) and current–voltage relationships. Membrane potential was held at 0 mV for 200 ms and alternated between ± 80 mV for 500 ms, current voltage relationships being determined where indicated.

Kinin stimulation of whole cell currents in mIMCD-K2 cells

Figure 4 shows the effect of repeated additions of 100 nM bradykinin upon whole-cell conductance; bradykinin stimulates a rapid peak increase in both inward and outward current at ± 80 mV is followed by a secondary peak and decline towards pre-stimulation values. Note that the increase in outward current is more pronounced than inward current, especially during the secondary phase (compare Figure 4b,c). Using a maximal dose of bradykinin (5 μM), an increase in whole cell conductance at ± 80 mV was from 16.9 ± 4.6 and -8.3 ± 3.9 pA pF^{-1} to 50.4 ± 9.8 and -50.1 ± 7.1 pA pF^{-1} ($n = 5$) respectively. With the membrane potential held at 0 mV, activation by bradykinin is associated with a decrease in the small outward current towards zero (Figure 4). This is therefore consistent with bradykinin activation of a Cl^- conductance. The Cl^- selective nature of this increased whole cell-conductance was further tested by reducing the bath Cl^- by 10 fold using aspartate as the substitute anion, in this case the reversal potential shifted in a positive direction by 35.5 ± 1.0 mV and the outward current was reduced to 18.9 ± 4.1 pA pF^{-1}, $n = 3$, $P < 0.05$ without change in inward current -52.4 ± 3.9 pA . pF^{-1}. The magnitude of the peak increase in whole cell-conductance observed with bradykinin (from 0.16 ± 0.05 nS pF^{-1} to 0.63 ± 0.11 ns pF^{-1}, $n = 5$) is

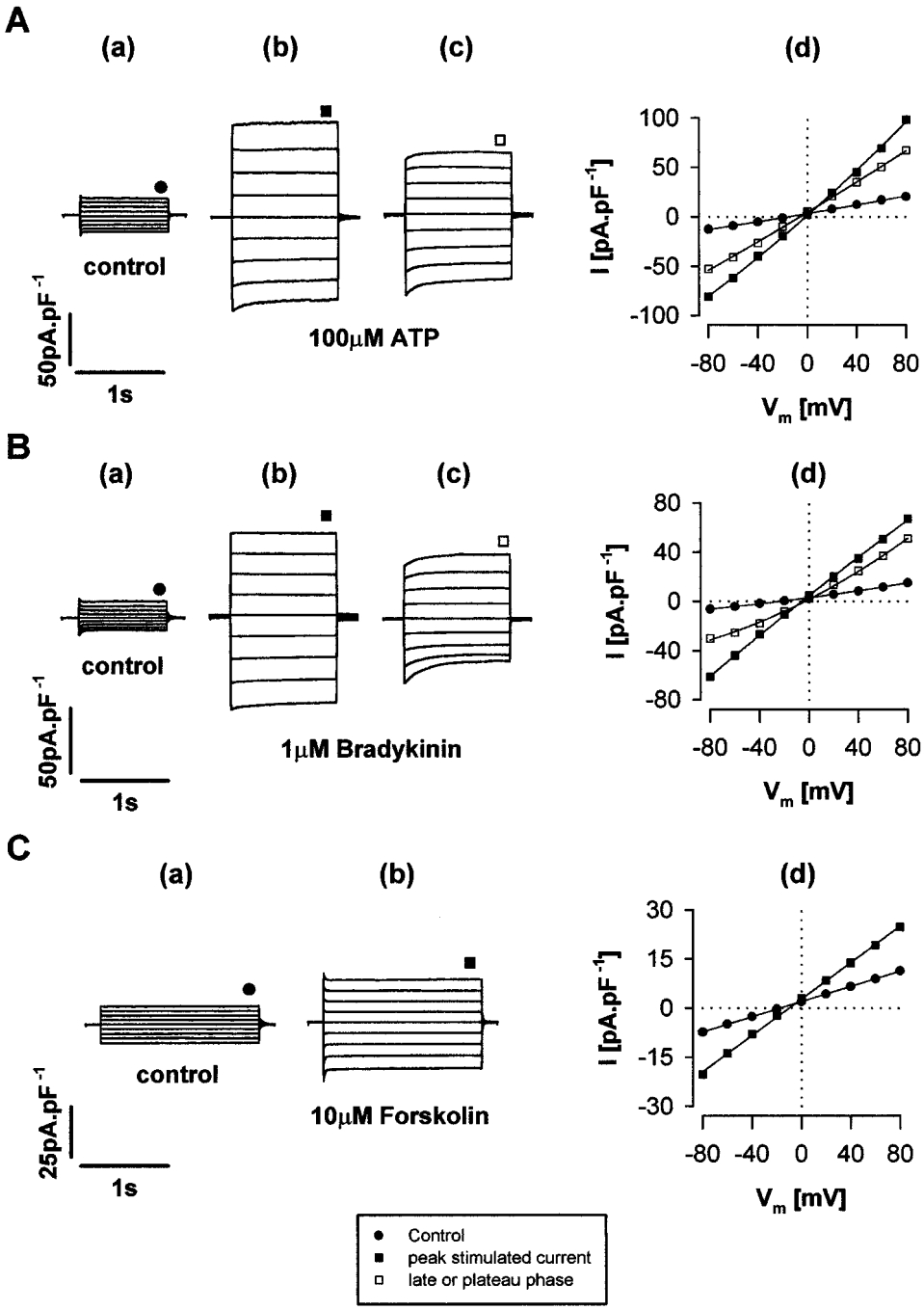

Figure 5 Comparison of the biophysical characteristics of the basal whole-cell currents with whole-cell currents stimulated by 100 μM ATP, 1 μM bradykinin and 100 μM forskolin. Plots of the I–V relationships of control and stimulated currents were measured at $\sim$1 s following voltage step, using a pulse protocol where the cell was held at 0 mV and pulsed to voltages between ± 80 mV for 1 s.

similar to that seen with exogenous ATP (100 μM) where whole cell conductance was increased from 0.12 ± 0.02 nS pF^{-1} to 0.72 ± 0.09 ns pF^{-1}) (see also Boese *et al*., 2000). Figure 5 compares the biophysical characteristics of the Cl^- conductance stimulated by bradykinin with that stimulated by ATP (100 μM) and by forskolin (100 μM) (CFTR). Whereas the CFTR-mediated increase in whole-cell current displays a linear, time-independent current/voltage relationship (Figure 5C), the currents activated by bradykinin (Figures 4b,c, and 5B) show a more complex behaviour. At intermediate levels of activation the bradykinin currents display distinct time-dependence with activation at positive potentials and inactivation at negative potentials giving rise to a slight outward rectification in the steady-state current voltage relationship (Figures 4c and 5B(c)). In contrast at higher levels of current density, the whole-cell currents display less inactivation and activation and the current-voltage relationship is approximately linear (Figures 4b and 5B(b)). This behaviour is identical to that seen for the ATP-activated whole cell currents (compare Figure 5A and B) and for those activated by ionomycin (Boese *et al*., 2000) in mIMCD-K2 cells. The kinetics of the whole-cell Cl^- selective currents activated by bradykinin at different levels of $[Ca^{2+}]_i$ are typical of $[Ca^{2+}]$-activated Cl^- channels in *Xenopus* oocytes (Kuruma & Hartzell, 2000).

Expression of mClCA1 mRNA and related transcripts in mIMCD-K2 cells

We have used an RT–PCR approach to demonstrate expression of mCLCA1 mRNA in mIMCD-K2 cells. Using gene-specific primers (Gruber *et al*., 1998b) to amplify reverse-transcribed mRNA, we identified a PCR product of ~518 bp consistent with mCLCA1 (mCACC) mRNA expression in mIMCD-K2 epithelial cells (Figure 6), (Romio *et al*., 1999; Gandhi *et al*., 1998), as well as in mouse kidney (Boese *et al*., 2000). Control reactions (water alone or minus reverse transcriptase) confirm specificity and lack of genomic DNA contamination. We have now obtained additional information on the PCR product(s) in mIMCD-K2 cells by cloning and sequencing: Figure 7 shows a multiple sequence alignment comparison between the 518 bp PCR product and both mCLCA1 and the mammary form, mCLCA2 (Accession numbers: U36445, Romio *et al*., 1999; AF047838, Gandhi *et al*., 1998; 96.7% identity, 501/518 bp, no gaps, AF108501, Lee *et al*., 1999; 502/518 bp no gaps, 96.9% identity, respectively Altschul *et al*., 1997), however, as can be seen in Figure 7, an additional but distinct transcript (527b) was identified by cloning. The additional transcript was not only distinct from mCLCA1 but also from the recently identified mammary transcript, mCLCA2,

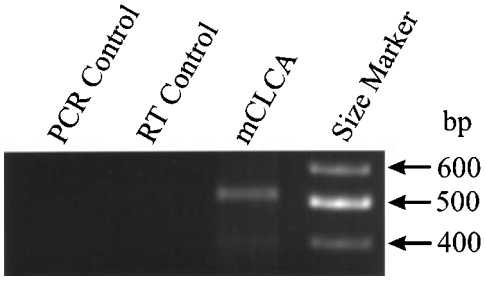

Figure 6 Identification of mCLCA expression in mIMCD-K2 cells. Ethidium-stained agarose gel showing an RT–PCR product using gene specific primers for mCLCA. Controls were water alone (PCR control) and omission of the reverse transcriptase (RT control).

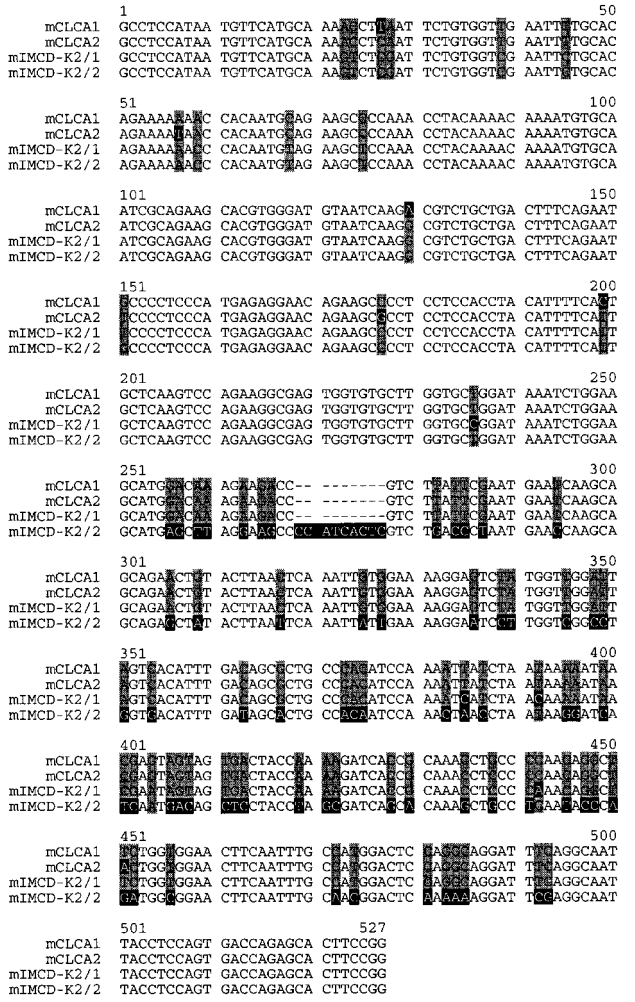

Figure 7 Alignment of the nucleotide sequences of the RT–PCR cDNA products from mIMCD-K2 cells (mIMCD-K2/1 and mIMCD-K2/2) with the known mouse CLCA homologues. Note that the mIMCD-K2/2 product contains an additional 9 bp insert compared to mCLCA1/2 at position 238, and that this product is divergent in sequence from mCLCA1/2 (83.3% identical to both mCLCA1/2).

Lee *et al*., 1999 (437/527 bp, 83.3% identity, 437/527, 83.3% identity respectively). Notably there is a 9 bp insert in the 527 bp product present in neither mCLCA1 or 2. Translation and comparison by multiple alignment of the predicted amino-acid sequence (Figure 8) of the two transcripts from mIMCDK2 cells with mCLCA1 and mCLCA2 demonstrates that the 518 bp product shares 162/172 amino acids in common with mCLCA1 (94.2% identity) and 161/172 amino acids in common with mCLA2 (93.6% identity). The similarity of the 527 bp PCR product is less (141/175, 80.6% identity compared to mCLCA1 and 140/175, 80% identity with mCLCA2) suggesting that this transcript is likely to arise from a new gene for an additional mCLCA family member. Alternatively, but less likely, the 527 bp product may represent an alternatively spliced variant of mCLCA1/2.

Discussion

We have used the mIMCD-K2 cell-line as an appropriate *in vitro* model of the inner medullary collecting duct. The mIMCD-K2 cell-line was established from initial half of the

Figure 8 Predicted amino-acid sequences of the CLCA sequences from mIMCD-K2 cells compared to known mouse CLCA homologues. Note that for both mIMCD-K2 RT–PCR products only one open-reading frame was evident. A = motif for a PKA consensus site, C = motif for a PKC consensus site. Note that an additional PKC site (position 143–145, STK) is present for the mIMCD-K2/2 product. Solid line indicates the location of a motif for a transmembrane G-protein-coupled receptor segment contained in the mIMCD-K2/2 product (PRINTS, Attwood *et al*., 1999, GPCRHODOPS family of motifs).

inner medulla from mice transgenic for SV40 from cells and homogeneity ensured by clonal dilution (Kizer *et al*., 1995). When grown as epithelial layers on confluent culture supports mIMCD-K2 epithelia are capable of electrogenic apical to basal Na^+ absorption stimulated by mineralocorticoid and sensitive to inhibition by amiloride and by atrial natriuretic hormone (Kizer *et al*., 1995; Green *et al*., 1996). In the culture conditions chosen for the present study, (no mineralocorticoids present), transepithelial Na absorption is minimized (Boese *et al*., 2000). mIMCD-K2 cells also display transepithelial anion secretion stimulated by arginine vasopressin or forskolin *via* cyclic AMP (Kizer *et al*., 1995; Boese *et al*., 2000). Anion secretion by mIMCD-K2 cells involves uphill accumulation of Cl^- and HCO_3^- across the basolateral membrane followed by downhill movement across the apical membrane. The nature of the apical Cl^- exit pathway has been studied by Vandorpe *et al*. (1995) who demonstrated CPT–cyclic AMP activated whole-cell currents consistent with CFTR. In addition, CFTR mRNA was identified using an RT–PCR approach. The CFTR conductance is unlikely to be the sole Cl^- conductance present as we have recently shown expression of a Cl^- conductance activated by exogenous ATP and by ionomycin *via* intracellular Ca^{2+}, that is distinct from CFTR on the basis of its biophysical properties (Boese *et al*., 2000).

The current data show that in addition to the properties already described, functional bradykinin B2 receptors are retained at both epithelial surfaces of mIMCD-K2 epithelia and that these are coupled to mobilization of $[Ca^{2+}]_i$, *via* release from intracellular stores. The ability of IMCD epithelia to respond to kinins released intraluminally and from the medullary interstitium is a feature substantiated by localization of kinin-B2 receptors in native tissue and by functional studies in primary cultured pig collecting duct cells (Cuthbert *et al*., 1985) and MDCK cells (Simmons, 1992).

The effects of kinins upon renal function are complex since both vascular and epithelial functions are affected. Infusion of kinins induces natriuresis in the absence of alteration of glonerular filtration rate. Functional analysis of kallikrein in mouse transgenic models demonstrates that secretion of human kallikrein in mouse plasma to levels 10–40 fold above normal render the transgenic animals chronically hypotensive (Song *et al*., 1996; Chao & Chao, 1996). This hypotensive effect can be reversed by aproptinin, a potent kallikrein inhibitor, or the bradykinin B2 specific receptor antagonist HOE-140. In humans it is also now apparent that a component of the hypotensive action of angiotensin-converting enzyme inhibitors (ACE) is mediated by potentiation of intra-renal kinins since HOE 140 significantly attenuates ACE-mediated hypotension in both normotensive and hypertensive individuals (Gainer *et al*., 1998).

The cellular mechanism underlying kinin-mediated hypotension or kinin-stimulated natriuresis remains controversial. In all studies using isolated renal epithelial layers, a consistent finding has been that of activation of transepithelial anion secretion. In the seminal studies of Cuthbert *et al*. (1985) the response of primary cultured pig papillary epithelia to kinins is activation of inward I_{sc} that is abolished in Cl^--free media. Furthermore this response to kinins is direct, and not mediated by release of prostanoids since piroxican does not affect kinin stimulation (Cuthbert *et al*., 1985; Simmons, 1992). The present data substantiate these findings in that bradykinin receptor B2-mobilization of intracellular Ca^{2+} is directly correlated with activation of transepithelial anion secretion. Our new finding is that this cellular response may be explained by the presence of an apical Ca^{2+}-activated Cl^- conductance and that this participates in transepithelial Cl^- secretion.

Properties of the Ca^{2+}-activated Cl^- conductance activated by bradykinin in mIMCD-K2 cells

The evidence that a Ca^{2+}-activated Cl^- conductance is the key membrane conductance activated by kinins in intact mIMCD-K2 epithelia is that (i) bradykinin causes transient mobilization of intracellular Ca^{2+} *via* B2 receptors at both epithelial surfaces and that this is directly correlated with transient activation of transepithelial Cl^- secretion; (ii) the Cl^--selective whole-cell currents activated by bradykinin show identical features to transepithelial events; and (iii) the biophysical properties of Cl^--selective whole-cell currents are quite distinct from those activated by forskolin (CFTR) but are identical to those activated by ionomycin (Boese *et al*., 2000). Ionomycin causes a sustained increase in intracellular Ca^{2+} and also causes a sustained activation of Cl^--selective whole-cell currents (Boese *et al*., 2000). The magnitude of the Ca^{2+}-activated Cl^- conductance is comparable to that observed for cyclic AMP-activated Cl^- conductance (CFTR); basal currents are increased approximately 4 fold by bradykinin (to 0.6 nS pF^{-1}). These values are also similar to Ca^{2+}-activated Cl^--activated Cl^- conductances observed in mouse pancreatic duct cells, where this conductance may be the primary route for Cl^- secretion across the apical membrane (Gray *et al*., 1994; Winpenny *et al*., 1995; 1998). The characteristics of the Ca^{2+}-activated whole cell Cl^- current stimulated by bradykinin were (1) a slightly outwardly rectifying current/voltage relationship at steady state, and (2) time and voltage dependence with slow activation during depolarization and slow inactivation during hyperpolarization. It should be noted that the kinetics of Ca^{2+}-activated whole cell Cl^- conductance depend upon the magnitude of the current stimulated and thus $[Ca^{2+}]_i$. It has been described by Evans & Marty (1986) that at 0.5 μM internal Ca^{2+}, large relaxations in current amplitude were observed and that the current voltage relationship was markedly rectifying, whereas at 2.0 μM Ca^{2+}, a time dependent decrease was smaller and the current voltage relationship was virtually linear (Evans & Marty, 1986). This dependence of the kinetics of the Ca^{2+}-activated Cl^-

conductance upon the amplitude of the Ca^{2+} signal has been explained by an apparent voltage dependence of the Ca^{2+}-sensitivity of the channel in *Xenopus* oocytes (Kuruma & Hartzell, 2000).

The biophysical characteristics of Ca^{2+}-activated Cl^- currents allow for differing physiological actions dependent upon the magnitude of the membrane potential and of the Cl^- electrochemical gradient. Thus activation of Ca^{2+}-activated Cl^- currents may mediate inward (depolarizing) or outward (hyperpolarizing) currents in the same cell, at different membrane potentials (Hume *et al*., 2000). As noted in the introduction, both inward and outward currents stimulated by bradykinin have been noted in IMCD primary cultured epithelial layers. The mIMCD-K2 cells in the present report do not express significant apical Na^+ conductance since they are cultured in the absence of mineralocorticoid, it is likely that only inward (secretory) currents will be present. However in the presence of significant Na^+ conductance at the apical membrane, the apical cell membrane potential may be held towards E_{Na} and inward currents generated.

Molecular identity of whole-cell Cl^- currents

Using homology cloning from the bovine tracheal Ca^{2+}-activated Cl^--activated Cl^- conductance sequence (Cunningham *et al*., 1995), Gandhi *et al*. (1998) were able to identify a mouse homologue (mCLCA1) from a mouse lung cDNA library. It is likely that mCLCA1 is a member of a family of related proteins. A new gene, mCLCA2, present in mammary gland has been recently described (Lee *et al*., 1999). The tissue-specific pattern of expression of each family member may be different in human tissues (Angel *et al*., 1999; Gruber *et al*., 1998a; 1999). Northern analysis has revealed expression of mCLCA1 in heart, lung, liver and kidney (Gandhi *et al*., 1998). The analysis of the tissue distribution of mCLCA1 was further investigated by Gruber *et al*. (1998b) by *in situ* hybridization, RT–PCR analyses and Northern blotting. mCLCA1 was strongly expressed in mouse secretory tissue such as mammary gland, respiratory, and intestinal epithelial but also in other epithelial tissue including kidney, uterus and epididymis. Another analysis of mCLCA1 distribution showed restricted expression to skin and kidney (Romio *et al*., 1999). We have already reported identification of an RT–PCR product with strong homology to mCLCA1 from mIMCD-K2 cell mRNA. Our present data further identify an additional transcript that shows significantly less identity to either mCLCA1 or the mammary form mCLCA2.

The structure and membrane topiology of CLCA proteins remains in doubt; Gruber *et al*. (1999) using hCLCA2 suggest that the primary 120 kD translation product is cleaved into two cell surface glycoproteins of 86 and 34 kD. In this model the 86 kD product is predicted to possess three transmembrane (TM) segments whereas the 34 kD product 2 TM segments. However this model is different from that proposed by the same group for hCLCA1 (Gruber *et al*., 1998a), and as noted by Romio *et al*. (1999) conservative prediction of transmembrane (TM) segments indicates only a single TM segment. Translation to amino-acid of the sequences identified in the present report (mCLCA1 235-410) (Figure 8) encompasses the first TM (hCLCA2 model) and includes the major cytosolic portion between TM1–TM2. Protein motif analysis (PRINTS, Attwood *et al*., 1999) of the mIMCDK2/2 product, however, identifies a TM motif (RRVVCLVLDkSGSMSLGSPITR) with significant homology to the rhodopsin-like GPCR superfamily 7-element motifs. This motif is not found in either mCLCA1 or mCLCA2 and suggests a different membrane topology to that proposed for mCLCA1 or hCLCA2. The reason for the existence of multiple transcripts of mCLCA in mIMCD-K2 cells is presently unknown. Direct experiments to ablate expression of each transcript with the existence of the Ca^{2+}-activated Cl^- conductance in these cells are now required.

The functional properties of mCLCA1 have been investigated by heterologous expression in HEK cells (Gandhi *et al*., 1998) and in *Xenopus* oocytes (mCACC, Romio *et al*., 1999). In HEK cells, calcium dependent currents were activated by inclusion of 2 mM Ca^{2+} in the pipette during 'fast' whole cell patch-clamp recording, or by ionomycin treatment. These Ca^{2+}-activated Cl^- currents were outwardly rectifying, but time independent, showing no characteristic activation on depolarization or inactivation on hyperpolarization. In *Xenopus* oocytes, in the absence of ionophore, mCACC expression was associated with elevation of an outwardly-rectifying time independent Cl^- current. Taken together, these data suggest that further work is required to relate the multiple protein products processed from a single gene (Gandhi *et al*., 1998), or multiple gene products to the biophysical properties of Ca^{2+}-activated Cl^- channels recorded in native tissue such as the inner medullary collecting duct. Finally, since the CLCA family shows significant homology to cell adhesion molecules (Cunningham *et al*., 1995), the possibility that mCLCA1 is not itself a Cl^- channel but a Cl^- channel regulator remains open.

Modulation of natriuresis by activation of apical Cl^- conductances in mIMCD-K2 cells

A number of agents have been reported to raise intracellular Ca^{2+} in IMCD cells; possible agonists include nucleotides such as ATP, UTP, kinins, acetylcholine adrenaline/noradrenaline and inflammatory cytokines (Zeidal, 1993; Simmons, 1993; Husted, 1998). Recently McCoy *et al*. (1999) have studied the actions of exogenous nucleotides upon ion transport by mIMCD-K2 cells. Both ATP and UTP acting *via* P2X and P2Y receptors inhibit Na^+ absorption and importantly stimulate Cl^- secretion. Our own data (Boese *et al*., 2000) show that ATP mobilizes intracellular Ca^{2+}, stimulates anion-dependent I_{sc} *via* the Ca^{2+}-activated Cl^- conductance. It is thus likely that a wide variety of hormonal and paracrines can activate apical Cl^- conductance *via* mobilization of intracellular Ca^{2+}. It is also important to note that bradykinin is likely to activate prostaglandin synthesis. *In vivo* renomedullary interstitital cells possess bradykinin receptors and are likely to release prostanoids in the vicinity of the collecting ducts (Siragy *et al*., 1997). Thus activation of CFTR *via* cyclic AMP, together with the Ca^{2+}-activated Cl^- conductance, will constitute the co-ordinate response to a number of diverse agents (see Simmons, 1993). In MDCK epithelia it is likely that activation of a Ca^{2+}-activated basolateral K^+ conductance also contributes to maximising secretion by cell hyperpolarization (Simmons, 1992; 1993).

We conclude that a number of natiuretic agents may act on IMCD *via* activation of a Ca^{2+}-activated Cl^- conductance, and that as such it may provide a new target for pharmacological manipulation of urinary NaCl output.

This work was supported by grants from the British Heart Foundation (M Glanville, NL Simmons), the Wellcome Trust (MA Gray, SH Boese and NL Simmons) and the Turkish Government (H Kose, CDA Brown).

References

ALTSCHUL, S.F., MADDEN, T.L., SCHAFFER, A.A., ZHANG, J.Z.Z., MILLER, W. & LIPMAN, D.J. (1997). Gapped BLAST and PSI-BLAST: a new generation of protein database search programs. *Nucleic Acid Res.,* **25,** 3389 – 3402.

ANGEL, M., VERMAT, T. & CULOUSCOU, J.-M. (1999). Identification of three novel members of the calcium-dependent chloride channel (CaCC) family predominantly expressed in the digestive tract and trachea. *FEBS Lett.,* **455,** 295 – 301.

ATTWOOD, T.K., FLOWER, D.R., LEWIS, A.P., MABEY, J.E., MORGAN, S.R., SCORDIS, P., SELLEY, J.N. & WRIGHT, W. (1999). PRINTS prepares for the new millennium. *Nucleic Acids Res.,* **27,** 220 – 225.

BOESE, S.H., GLANVILLE, M., AZIZ, O., GRAY, M.A. & SIMMONS, N.L. (2000). Ca^{2+} and cAMP-activated Cl^- conductances mediate Cl^- secretion in a mouse renal inner medullary collecting duct cell line. *J. Physiol.,* **523,** 325 – 338.

CHAO, J. & CHAO, L. (1996). Functional analysis of human tissue kallikrein in transgenic mouse models. *Hypertension,* **27,** 491 – 494.

CORPET, F. (1988). Multiple sequence alignment with hierarchical clustering. *Nucleic Acids Res.,* **16,** 10881 – 10890.

CUNNINGHAM, S.A., AWAYDA, M.S., BUBIEN, J.K., ISMAILOV, I.I., ARRATE, M.P., BERDIEV, B.K., BENOS, D.J. & FULLER, C.M. (1995). Cloning of an epithelial chloride channel from bovine trachea. *J. Biol. Chem.,* **270,** 31016 – 31026.

CUTHBERT, A.W., GEORGE, A.M. & MCVINISH, L. (1985). Kinin effects on electrogenic ion transport in primary cultures of pig renal papillary collecting duct cells. *Am. J. Physiol.,* **249,** F439 – F447.

EVANS, M.G. & MARTY, A. (1986). Calcium-dependent chloride currents in isolated cells from rat lacrimal glands. *J. Physiol.,* **378,** 437 – 460.

FIGUEROA, C.D., GONZALES, C.B., GRIGORIEV, S., ALLA, S.A., HAASEMANN, M., JARNAGIN, K. & MULLER-ESTERL, W. (1995). Probing for the bradykinin B2 receptor in rat kidney by anti-peptide and anti-ligand antibodies. *J. Histochem. Cytochem.,* **43,** 137 – 148.

GAINER, J.V., MORROW, J.D., LOVELAND, A., KING, D.J. & BROWN, N.J. (1998). Effect of bradykinin-receptor blockade on the response to angiotensin-converting-enzyme inhibitor in normotensive and hypertensive subjects. *New Engl. J. Med.,* **18,** 1285 – 1292.

GANDHI, R., ELBLE, R.C., GRUBER, A.D., SCHREUR, K.D., JI, H.L., FULLER, C.M. & PAULI, B.U. (1998). Molecular and functional characterization of a calcium-sensitive chloride channel from mouse lung. *J. Biol. Chem.,* **273,** 32096 – 32101.

GRAY, M.A., WINPENNY, J.P., PORTEUS, D.J., DORIN, J.R. & ARGENT, B.E. (1994). CFTR and calcium-activated chloride currents in pancreatic duct cells of a transgenic CF mouse. *Am. J. Physiol.,* **266,** C213 – C221.

GREEN, R.B., SLATTERY, M.J., GIANFERRARI, E., KIZER, N.L., MCCOY, D.E. & STANTON, B.A. (1996). Hyperosmolarity inhibits sodium absorption and chloride secretion in mIMCD-K2 cells. *Am. J. Physiol.,* **271,** F1248 – F1254.

GRUBER, A.D., ELBLE, R.C., HONG-LONG, J., SCHREUR, K.D., FULLER, C.M. & PAULI, B.U. (1998a). Genomic cloning, Molecular characterization and functional analysis of human CLCA1, the first human member of the family of Ca^{2+}-activated Cl^- channel proteins. *Genomics,* **54,** 200 – 214.

GRUBER, A.D., GANDHI, R. & PAULI, B.U. (1998b). The murine calcium-sensitive chloride channel (mCACC) is widely expressed in secretory epithelia and other select tissues. *Histochem. Cell Biol.,* **110,** 43 – 49.

GRUBER, A.D., SCHREUR, K.D., HONG-LONG, J., FULLER, C.M. & PAULI, B.U. (1999). Molecular cloning and transmembrane structure of hCLCA2 from human lung, trachea and mammary gland. *Am. J. Physiol.,* **276,** C1261 – C1270.

GRYNKIEWICZ, G., POENIE, M. & TSEIN, R.Y. (1985). A new generation of Ca^{2+} indicators with greatly improved fluorescence properties. *J. Biol. Chem.,* **260,** 3440 – 3450.

HAMILL, O.P., MARTY, A., NEHER, E., SAKMANN, B. & SIGWORTH, F.J. (1981). Improved patch-clamp techniques for high-resolution current recording from cells and cell-free membrane patches. *Pflugers Archiv.,* **391,** 85 – 100.

HUME, J.R., DUAN, D., COLLIER, M.L., YAMAZAKI, J. & HOROWITZ, B. (2000). Anion transport in Heart. *Phys. Rev.,* **80,** 31 – 81.

HUSTED, R.F. & STOKES, J.B. (1996). Separate regulation of Na and anion transport by IMCD: location, aldosterone, hypertonicity, TGF-beta1 and cAMP. *Am. J. Physiol.,* **271,** F433 – F439.

HUSTED, R.F., VOLK, K.A., SIGMUND, R.D. & STOKES, J.B. (1995). Anion secretion by the inner medullary collecting duct. *J. Clin. Invest.,* **95,** 644 – 650.

HUSTED, R.F., ZHANG, C. & STOKES, J.B. (1998). Concerted actions of IL-1beta inhibit Na absorption and stimulate anion secretion by IMCD cells. *Am. J. Physiol.,* **275,** F946 – F954.

KIZER, N.L., LEWIS, B. & STANTON, B.A. (1995). Electrogenic sodium absorption and chloride secretion by an inner medullary collecting duct cell line (mIMCD-K2). *Am. J. Physiol.,* **268,** F347 – F355.

KUMURA, A. & HARTZELL, H.C. (2000). Bimodal control of a Ca^{2+} activated Cl^- channel by different Ca^{2+} signals. *J. Gen. Physiol.,* **115,** 59 – 80.

LEE, D., HA, S., KHO, Y., KIM, J., CHO, K., BAIK, M. & CHOI, Y. (1999). Induction of mouse Ca^{2+}-sensitive chloride channel2 gene during involution of mammary gland. *Biochem. Biophys. Res. Comm.,* **264,** 933 – 937.

MARGOLIUS, H.S. (1984). The kallikrein-kinin system and the kidney. *Ann. Rev. Physiol.,* **46,** 309 – 326.

MCCOY, D.E., TAYLOR, A.L., KUDLOW, B.A., KARLSON, K., SLATTERY, M.J., SCHWIEBERT, L.M., SCHWIEBERT, E.M. & STANTON, B. (1999). Nucleotides regulate NaCl transport in mIMCD-K2 cells via P2X and P2Y purinergic receptors. *Am. J. Physiol.,* **277,** F552 – F559.

MUKAI, H., FITZGIBBON, W.R., BOZEMAN, G., MARGOLIUS, H.S. & PLOTH, D.W. (1996). Bradykinin B2 receptor antagonist increases chloride and water absorption in rat medullary collecting duct. *Am. J. Physiol.,* **271,** R352 – R360.

ROCHA, A.S. & KUDO, L.H. (1990a). Atrial peptide and cGMP effects on NaCl transport in inner medullary collecting duct. *Am. J. Physiol.,* **259,** F265 – F268.

ROCHA, A.S. & KUDO, L.H. (1990b). Factors governing sodium and chloride transport across the inner medullary collecting duct. *Kid. Int.,* **38,** 654 – 667.

ROMIO, L., MUSANTE, L., CINTI, R., SERI, M., MORAN, O., ZEGARRA-MORAN, O. & GALIETTA, L.J.V. (1999). Characterisation of a murine gene homologous to the bovine CACC chloride channel. *Gene,* **228,** 181 – 188.

SCHANSTRA, J.P., ALRIC, C., MARIN-CASTANO, M.E., GIROLAMI, J.P. & BASCANDS, J.L. (1999). Renal bradykinin receptors: Localisation, transduction pathways and molecular basis for a possible pathological role. *Int. J. Mol. Med.,* **3,** 185 – 191.

SCHWIEBERT, E.M., LOPES, A.G. & GUGGINO, W.B. (1994). Chloride channels along the nephron. *Curr. Top. Membr.,* **42,** 265 – 315.

SIMMONS, N.L. (1992). Acetylcholine and kinin augmentation of Cl^- secretion by prostaglandin E_1 in a canine renal epithelial cell-line (MDCK). *J. Physiol.,* **447,** 1 – 15.

SIMMONS, N.L. (1993). Renal epithelial Cl^- secretion. *Exp. Physiol.,* **78,** 117 – 137.

SIRAGY, H.M., JAFFA, A.A. & MARGOLIUS, H.S. (1997). Bradykinin B2 receptor receptor modulates renal prostaglandin E2 and nitric oxide. *Hypertension,* **29,** 757 – 762.

SONG, Q., CHAO, J. & CHAO, L. (1996). High level of circulating human tissue kallikrein induces hypotension in transgenic mouse model. *Clin. Exp. Hypertension,* **18,** 975 – 993.

VANDORPE, D.H., CIAMPOLILLO, F., GREEN, R.B. & STANTON, B.A. (1997). Cyclic nucleotide-gated cation channels mediate sodium absorption by IMCD (mIMCD-K2) cells. *Am. J. Physiol.,* **272,** C901 – C910.

VANDORPE, D., KIZER, N., CIAMPOLLILO, F., MOYER, B., KARLSON, K., GUGGINO, W.B. & STANTON, B.A. (1995). CFTR mediates electrogenic chloride secretion in mouse inner medullary collecting duct (mIMCD-K2) cells. *Am. J. Physiol.,* **269,** C683 – C689.

VIO, C.P., OLAVARRIA, V., GONZALES, C., NAZAL, L., CORDOVA, M. & BALESTRINI, C. (1998). Cellular and functional aspects of the renal kallikrein system in health and disease. *Biol. Res.,* **31,** 305 – 322.

WINPENNY, J.P., HARRIS, A., HOLLINGSWORTH, M.A., ARGENT, B.E. & GRAY, M.A. (1998). Calcium-activated chloride conductance in a pancreatic adenocarcinoma of ductal origin (HPAF) and in freshly isolated human pancreatic duct cells. *Pflügers Archiv.,* **435,** 796 – 803.

WINPENNY, J.P., VERDON, B., MCALROY, H.L., COLLEDGE, W.H., RATCLIFF, R., EVANS, M.J., GRAY, M.A. & ARGENT, B.E. (1995). Calcium-activated chloride conductance is not increased in pancreatic duct cells of CF mice. *Pflügers Archiv.,* **430,** 26–36.

WIRTH, K., HOCK, F.J., ALBUS, U., LINZ, W., ALPERMANN, H.G., ANAGNOSTOPOULOS, H., HENKE, S.T., BREIPOHL, G., KONIG, W., KNOLLE, J. & SHOLKENS, B.A. (1991). Hoe 140, a new potent and long acting bradykinin antagonist; in vivo studies. *Br. J. Pharmacol.,* **102,** 774–777.

ZEIDEL, M.L. (1993). Hormonal regulation of inner medullary collecting duct sodium transport. *Am. J. Physiol.,* **265,** F159–F173.

(Received March 23, 2000
Revised August 1, 2000
Accepted October 2, 2000)